Neotropical Ichthyology

Original article

https://doi.org/10.1590/1982-0224-2023-0106

urn:lsid:zoobank.org:pub:970EB7E6-5A64-4A03-AEE3-81A4FB2D0E9F

A new species of *Aequidens* (Cichliformes: Cichlidae) from the rio Paraguai basin, Brazil

Rianne Caroline de Oliveira[1,2], Luiz Fernando Caserta Tencatt[3], Gabriel de Carvalho Deprá[1], Ricardo Britzke[4], Claudio Oliveira[5] and Weferson Júnio da Graça[1,2,6]

Correspondence:
Rianne Caroline de Oliveira
rianne.oliveira@gmail.com

Morphological and molecular data support the description of a new *Aequidens* species from the upper rio Correntes, considered herein as endemic to the upper rio Paraguai basin in the Cerrado biome in Brazil. The new species is distinguished from all congeners, except from *A. plagiozonatus* by having anteriorly oblique dark brown flank bars *vs*. vertical flank bars, and is additionally distinguished from some congeners by showing a discontinuous lateral band and presence of a dark cheek spot. The new species differs from *Aequidens plagiozonatus* by having the profile of the dorsal part of head almost straight (in lateral view), with a conspicuous concavity at the interorbital, and by the longer length of upper and lower jaws. Furthermore, delimitation analyses based on mitochondrial data provide additional support for the validity of the species. Our study data also revealed the occurrence, and consequently the first record, of *A. plagiozonatus* in the upper rio Araguaia basin, which was most likely driven by headwater capture events.

Keywords: Cerrado biome, DNA barcode, Molecular data, Morphological data, Species delimitation.

Submitted September 23, 2023
Accepted April 4, 2024
by Hernán López-Fernández
Epub June 10, 2024

1 Núcleo de Pesquisas em Limnologia, Ictiologia e Aquicultura, Centro de Ciências Biológicas, Universidade Estadual de Maringá, Av. Colombo, 5790, 87020-900 Maringá, PR, Brazil. (RCO) rianne.oliveira@gmail.com (corresponding author), (GCD) gabrieldepra@gmail.com, (WJG) weferson@nupelia.uem.br.

2 Programa de Pós-Graduação em Ecologia de Ambientes Aquáticos Continentais, Departamento de Biologia, Centro de Ciências Biológicas, Universidade Estadual de Maringá, Av. Colombo, 5790, 87020-900 Maringá, PR, Brazil.

3 Departamento de Biologia e Zoologia, Instituto de Biociências, Universidade Federal de Mato Grosso, Av. Fernando Corrêa da Costa, 2367, Boa Esperança, 78060-900 Cuiabá, MT, Brazil. (LFCT) luiztencatt@hotmail.com.

4 Museo de Historia Natural, Universidad Nacional Mayor de San Marcos, Av. Gral. Antonio Alvarez de Arenales 1256, Jesús María 15072, Lima, Peru. (RB) rbritzke@unmsm.edu.pe.

5 Departamento de Biologia Estrutural e Funcional, Instituto de Biociências, Universidade Estadual Paulista, R. Prof. Dr. Antonio C. W. Zanin 250, 18618-689 Botucatu, SP, Brazil. (CO) claudio.oliveira@unesp.br.

6 Programa de Pós-Graduação em Biologia Comparada, Centro de Ciências Biológicas, Universidade Estadual de Maringá, Av. Colombo, 5790, 87020-900 Maringá, PR, Brazil.

Online version ISSN 1982-0224
Print version ISSN 1679-6225

Neotrop. Ichthyol.
vol. 22, no. 2, Maringá 2024

Dados morfológicos e moleculares apoiam a descrição de uma nova espécie de *Aequidens* do alto rio Correntes, considerada aqui como uma espécie endêmica da bacia do alto rio Paraguai, no bioma Cerrado no Brasil. A nova espécie distingue-se de todas as congêneres, exceto de *Aequidens plagiozonatus*, por apresentar barras laterais marrom-escuras oblíquas em direção anterodorsal *vs.* barras verticais nos flancos. Além disso, distingue-se de algumas espécies por apresentar uma faixa lateral descontínua e pela presença de uma mancha escura na porção entre a órbita e a margem preopercular. A nova espécie difere de *A. plagiozonatus* por apresentar o perfil da parte dorsal da cabeça (em vista lateral) aproximadamente reta, com uma concavidade conspícua na porção interorbital, e pelo maior comprimento das maxilas superior e inferior. Além disso, análises de delimitação baseadas em dados mitocondriais oferecem evidência a favor da validade da espécie. Nossos dados também revelaram a ocorrência e, consequentemente, o primeiro registro de *A. plagiozonatus* na bacia do alto rio Araguaia, provavelmente devido a eventos de captura de cabeceiras.

Palavras-chave: Bioma Cerrado, Dados moleculares, Dados morfológicos, Delimitação de espécies, DNA barcode.

INTRODUCTION

Cichlasomatini is a well-supported clade among the seven Cichlinae tribes proposed by Ilves *et al*. (2018; *viz*. Cichlini, Retroculini, Astronotini, Chaetobranchini, Geophagini, Cichlasomatini, and Heroini). However, some of the relationships within this tribe are still unclear. One of the most important issues related to Cichlasomatini is the monophyly of *Cichlasoma* Swainson, 1839 and *Aequidens* Eigenmann & Bray, 1894, the two oldest generic names inside Cichlasomatini. *Cichlasoma* is nested within *Aequidens* (Musilová *et al*., 2008; Ilves *et al*., 2018) resulting in a paraphyletic group. However, *Aequidens* is distinguished from *Cichlasoma* by morphological characteristics such as naked, rather than scaled dorsal and anal fins longer caudal peduncle with 2–3 vertebrae (2 or 0 in *Cichlasoma*), and 4–5 vertical bars from the midlateral spot to the caudal peduncle in *Aequidens* (6 in *Cichlasoma*) (Kullander, 1986). The uni or triserial predorsal squamation, the presence of a lateral band on the middle of the flank, and some meristic traits, such as a long peduncle with more vertebrae, are characteristics that differentiate *Aequidens* species from other Neotropical cichlid genera (Kullander, 1983, 1986; Kullander, Nijssen, 1989). The phenotypic character states used to distinguish species within *Aequidens* are mainly related to coloration, such as differences in the patterns of the longitudinal stripe and flank bars, cheek spot, and buccal stripes. The morphological characters traditionally used in species delimitation in *Aequidens* (and other Cichlasomatini as well) show a high degree of plasticity, such as meristic and morphometric. This makes the delimitation of the range of variation and, consequently the species delimitation, difficult and dependent on authoritative argumentation or evidence from other independent sources of data.

Aequidens comprises 17 valid species (Fricke *et al*., 2024) distributed in the rios Amazon-Orinoco-Guiana (AOG) region, and in the rio La Plata basin (Paraná-Paraguay) (Kullander, 2003; Hernández-Acevedo *et al*., 2015). The majority of *Aequidens* species were described from the Amazon-Orinoco-Guyana area (AOG region of van der Sleen, Albert, 2018). *Aequidens plagiozonatus* Kullander, 1984 is the only species known from the río La Plata basin (Paraná-Paraguay), occurring also in the rio Guaporé together with *A. viridis* (Heckel, 1840). The records of this species in other hydrographic basins are deemed non-native occurrences (Reis *et al*., 2020).

The rio Correntes is a tributary to the upper rio Paraguai basin draining the border regions of the Mato Grosso and Mato Grosso do Sul states, Central Brazil. In the surroundings of the city of Sonora, Mato Grosso do Sul, the river flows through a sinkhole (around 17°36'49"S 54°50'14"W) into a natural karst tunnel about 800 m long (SEMA, 2005). Along with the headwaters of the rio Araguaia basin upstream from Barra do Garças in Mato Grosso and the upper rio Taquari basin, also a tributary to the upper rio Paraguai basin, the upper rio Correntes basin (upstream the sinkhole) is part of one of the smallest endemic regions for Neotropical freshwater fishes (Dagosta *et al*., 2020). Currently, four species are known to be endemic to the upper rio Correntes basin: *Melanorivulus dapazi* (Costa, 2005), *Eigenmannia correntes* Campos-da-Paz & Queiroz, 2017, *Characidium chicoi* da Graça, Ota & Domingues, 2019, and *Cyphocharax caboclo* Melo, Tencatt & Oliveira, 2022.

During survey efforts in the rio Correntes basin (2018 to 2021), an undescribed species of *Aequidens* was captured exclusively in the upper portion of this basin (*i.e*., upstream from the sinkhole). In this paper, we combine morphological and molecular evidence to recognize and describe this new species of *Aequidens*, and discuss the occurrence of *A. plagiozonatus* in the rio Araguaia basin based on recent records in fish collections.

MATERIAL AND METHODS

Morphological data. Measurements and counts were obtained under a stereomicroscope, in accordance with Ota *et al*. (2021) and Deprá *et al*. (2022). The following measurements are included: preanal distance, from the premaxillary symphysis to the base of the first anal-fin spine; distance from dorsal to caudal fin, from the base of the first dorsal-fin spine to the vertical through distal margin of the hypurals, between the dorsal and ventral lobes; distance from dorsal to anal fin, from the base of the first dorsal-fin spine to the base of the first anal-fin spine; distance from dorsal to pelvic fin, from the base of the first dorsal-fin spine to the base of the pelvic-fin spine; distance from dorsal to pectoral fin, from the base of the first dorsal-fin spine to the base of the first pectoral-fin ray; caudal peduncle length (straight), from the vertical line through the base of the last dorsal-fin ray, on the intersection with the lower lateral line, to distal margin of the hypurals; caudal peduncle length (oblique), from the base of the last anal-fin ray to distal margin of the hypurals; dorsal-fin base length (spine), from the base of the first dorsal-fin spine to the base of the last dorsal-fin spine; dorsal-fin base length (total), from the base of the first dorsal-fin spine to the base of the last dorsal-fin ray; anal-fin base length (spine), from the base of the first anal-fin spine to the base of the last anal-fin spine; anal-fin base

length (total), from the base of the first anal-fin spine to the base of the last anal-fin ray. The series of scales between the dorsal-fin base and the upper lateral line were counted starting from: a) the scale reaching the base of the first spine (anterior series); and b) the scale reaching the base of the last spine (middle series). The scales on the lower lateral line are made up of the following: the number of scales to the distal end of hypurals plus the scales onto caudal fin (usually two scales). Counts from holotype are indicated by an asterisk. The counts are followed by their frequency in parentheses, unless when equal for all specimens. Measurements expressed as a percentage of head length.

Two specimens were cleared and stained (c&s) following the methodology of Taylor, Van Dyke (1985) for osteological examination. Vertebrae were counted as in Deprá *et al*. (2021). Fused PU1+U1 (pleural and ural vertebrae) was treated as a single bone. The lower pharyngeal tooth plate was examined as described by Barel *et al*. (1976).

We adopted the coloration-related terminology described by Říčan *et al*. (2005), which defined the homology and aspects of ontogeny of nine flank bars along the body. Specimens were deposited in the following Brazilian institutions: Coleção Ictiológica de Três Lagoas, Universidade Federal do Mato Grosso do Sul, Três Lagoas (CITL); Coleção Ictiológica do Núcleo de Pesquisas em Limnologia, Ictiologia e Aquicultura, Universidade Estadual de Maringá, Maringá (NUP); Coleção de Peixes da Universidade Federal do Mato Grosso, Cuiabá (CPUFMT); Museu de Ciências e Tecnologia, Pontifícia Universidade Católica do Rio Grande do Sul, Porto Alegre (MCP); Museu de Zoologia, Universidade Estadual de Londrina, Londrina (MZUEL); and Coleção do Laboratório de Biologia e Genética de Peixes da Universidade Estadual Paulista, Botucatu (LBP). To infer the IUCN criteria, the software GeoCAT (Geospacial Conservation Assessment Tool; http://geocat.kew.org) allowed the calculation of the Extent of Occurrence of the new species based on the currently known points of occurrence.

Molecular data. *Sampling and sequencing*. We obtained partial sequences of the cytochrome c oxidase subunit I (COI) gene of the new species, of *Aequidens plagiozonatus* from the Paraguai and rio Araguaia basins, and of *A. gerciliae* Kullander, 1995. The sequences of other *Aequidens* species were obtained from the GenBank database.

Voucher specimens were fixed in 10% formalin and then stored at 70º GL ethanol. Tissue samples were extracted from specimens prior to their fixation and preserved and stored at 95º GL ethanol. Total DNA was extracted following Ivanova *et al*. (2006). Subsequently, the DNA barcode region of the COI was amplified by polymerase chain reaction (PCR) using the primers FISH-F6 (5'-ACYAAYCACAAAGAYATTGGCA-3') and FISH-R7 (5'-TARACTTCTGGRTGDCCRAAGAAYCA-3') described by Jennings *et al*. (2019). The PCR was performed in a thermocycler with a final volume of 12.5 µl containing 7.85 µl distilled water (ddH2O), 0.30 µl deoxynucleotide triphosphate (dNTP) (2 mM), 1.25 µl PCR buffer (10×), 0.4 µl MgCl2 (50 mM), 0.25 µl each primer, 2 µL DNA (200 ng) and 0.20 µl Taq DNA polymerase PHT (Phoneutria). PCR was performed under the following conditions: an initial denaturation at 95 ºC for 5 min, followed by 30 cycles including denaturation at 95 ºC for 60 s, annealing (primer hybridization) at 52 ºC for 45 s and nucleotide extension at 68 ºC for 1 min, with a final extension at 68 ºC for 10 min. The PCR products were amplified and checked on a 1% agarose gel before being purified using ExoSAP-IT (USB Corporation, Cleveland, OH, USA) according to the manufacturer's protocol.

To sequence both DNA strands, the purified products were used as templates. Further, the cycle sequencing reaction was accomplished using a BigDye Terminator v. 3.1 Cycle Sequencing Ready Reaction kit (Applied Biosystems, Austin, TX, USA) in a final volume of 7 µl containing 0.1 µl of purified PCR product, 0.35 µl primer (10 mM), 1.05 µl buffer 5×, 0.7 µl BigDye mix and 3.9 µl distilled water. The final mixture of the purified PCR product was then purified again using ethanol precipitation and sequenced using the 3500-Genetic Analyzer (Applied Biosystems) at IBTEC, at the Instituto de Biociências at Universidade Estadual Paulista "Júlio de Mesquita Filho", UNESP, Botucatu.

Molecular analysis. Sequences of COI were obtained from nine specimens (two of the new species, six of *A. plagiozonatus* and one of *A. gerciliae*) and 16 additional sequences were obtained from GenBank, totalizing 25 sequences in the final matrix (23 of *Aequidens* and two of *Pterophyllum* Heckel, 1840). All sequences and GenBank accession numbers used in this study are described in Tab. **S1**. Species added to the analysis were: *Aequidens diadema* (Heckel, 1840) (rio Amazonas basin in Iquitos), *A. epae* Kullander, 1995 (rio Tapajós basin), *A. tetramerus* (Heckel, 1840) (French Guiana and Suriname), *A. pallidus* (Heckel, 1840) (rio Negro and Jatapu basins), *A. gerciliae* (rio Tapajós basin), *A. michaeli* Kullander, 1995 (rio Xingu basin), *Cichlasoma dimerus* (Heckel, 1840) (Lower rio Paraná basin), *C. orientale* Kullander, 1983 (Atlantic mid-north-eastern Rivers), *C. paranaense* Kullander, 1983 (Upper rio Paraná basin) and *C. sanctifranciscense* Kullander, 1983 (Atlantic mid-north-eastern Rivers). *Pterophyllum altum* Pellegrin, 1903 was added as the outgroup. For the sequences obtained from GenBank we followed the identification from original studies. Sequences were aligned using Clustal W algorithm (Thompson *et al*., 1994) incorporated in MEGA X (Kumar *et al*., 2018). In MEGA X, sequences were translated into amino acids for the verification for stop codons along the sequences, which were absent.

For species delimitation, four approaches were used: i) Poisson Tree Process analysis (PTP; Zhang *et al*., 2013); ii) General Mixed Yule Coalescent Model analysis (GMYC; Pons *et al*., 2006; Fujisawa, Barraclough, 2013); iii) Automatic Barcode Gap Discovery analysis (ABGD; Puillandre *et al*., 2012); and iv) Assemble Species by Automatic Partitioning (ASAP; Puillandre *et al*., 2021).

A maximum likelihood (ML) analysis was performed in MEGA-X v. 10.2.1 (Kumar *et al*., 2018) using the best nucleotide substitution model (K2+G, lowest BIC score: 4685,00 with 91 parameters), five random searches and 1,000 bootstrap replicates and other parameters at default, showing the best tree. The resulting ML tree was used as an input tree for PTP analysis performed on the PTP web server (species.h–its.org/server) using 500,000 MCMC generations with 0.1 burn-in rate.

For GMYC analysis, a Bayesian Inference analysis was performed to construct a phylogenetic tree, inserting the fasta file in BEAUTi (Drummond *et al*., 2012), selecting the HKY+G+I nucleotide evolutionary substitution model, the uncorrelated relaxed clock and the speciation birth-death model (Yule process), on an arbitrary timescale. A random tree was used as a starting tree for the MCMC searches with a run of 10 million generations, and a tree sampled every 1,000 generations and posteriorly running the analysis in BEAST v. 1.8.4 (Drummond *et al*., 2012). Following that, Tracer v. 1.7.2 (Rambaut *et al*., 2018) was used to investigate the distribution of log-likelihood scores and the identification of the stationary phase for each search (to determine whether

more runs were necessary to achieve convergence). In the burn-in procedure, the sampled topologies below the asymptote were removed (10%), and the remaining trees were used to construct a 50% majority-rule consensus tree in TreeAnnotator v. 1.8.4. (included in BEAST). The resulting ultrametric tree was displayed in FigTree v. 1.4.3 (Rambaut, 2019) and a newick archive exported was employed as an input file for the GMYC analysis done using a single threshold method at the GMYC webserver (species.h–its.org/gmyc/R).

The ABGD analysis (Puillandre *et al*., 2012) was performed on the ABGD web server (bioinfo.mnhn.fr/abi/public/abgd/abgdweb.html), inserting the fasta file with the aligned sequences, using Kimura (K2P; 2.0) distance model and other parameters at default (Pmin = 0.001; Pmax = 0.1). In addition, the ASAP analysis (Puillandre *et al*., 2021) was performed on the ASAP web server (https://bioinfo.mnhn.fr/abi/public/asap/asapweb.html), inserting the fasta file with the aligned sequences, using Kimura (K80; 2.0) distance model.

RESULTS

Aequidens pirilampo, new species

urn:lsid:zoobank.org:act:6F182F43-5BFE-46B4-B7DE-6580FE19C11F

(Figs. 1–5; Tab. 1)

Aequidens. —Melo *et al*., 2022:332 (Brazil, Mato Grosso, Ribeirão Comprido; first record).
Aequidens sp. —Gimênes, Rech, 2022:595 (Brazil, Mato Grosso, photo).

Holotype. NUP 23543, 94.7 mm SL, Brazil, Mato Grosso State, Itiquira Municipality, ribeirão Comprido, tributary of the rio Correntes, rio Paraguai basin, 17°32'04"S 54°25'36"W, 27 Jan 2021, L. F. C. Tencatt & M. N. Souza.

Paratypes. All from Brazil, rio Paraguai basin. **Mato Grosso State:** Itiquira Municipality: LBP 30742, 1, 42.1 mm SL, 18 Sep 2021, L. F. C. Tencatt, M. N. Souza & M. A. Alves; LBP 30743, 1, 48.3 mm SL, 5 Apr 2018, L. F. C. Tencatt, M. N. Souza & M. A. Alves; LBP 31524, 4, 41.8–94.0 mm SL, 18–21 Sep 2021, L. F. C. Tencatt, M. N. Souza & M. A. Alves, same data as holotype. MCP 54880, 4, 42.6–67.0 mm SL, MZUEL 22500, 4, 43.0–76.6 mm SL, NUP 23546, 5, 39.8–66.2 mm SL, NUP 23547, 2 c&s, 59.2–59.6 mm SL, collected with LBP 31524. NUP 21644, 9, 28.7–68.5 mm SL, córrego de Cima, tributary of the rio Correntes, 17°39'52"S 54°14'46"W, 31 Aug 2018, Nupélia staff. NUP 23544, 7, 14.9–87.2 mm SL, collected with holotype. **Mato Grosso do Sul State:** Sonora Municipality: CITL 392, 10, 24.5–74.5 mm SL, córrego de Baixo, tributary of the rio Correntes, 17°42'33"S 54°21'32"W, 7 Aug 2021, L. F. C. Tencatt, M. N. Souza, V. Carvalho & M. A. Alves. CITL 393, 4, 17.3–39.3 mm SL, unnamed stream, tributary of the rio Correntes, 17°35'42"S 53°53'33"W, 29 Dec 2020, L. F. C. Tencatt & M. N. Souza. CPUFMT 7763, 2, 64.8–66.1 mm SL, same data as CITL 392, 2 Oct 2021, L. F. C. Tencatt, M. N. Souza & M. A. Alves.

FIGURE 1 | *Aequidens pirilampo*, NUP 23543, 94.7 mm SL, holotype, Brazil, State of Mato Grosso, municipality of Itiquira, Comprido Creek, tributary of Correntes River, rio Paraguai basin.

Diagnosis. *Aequidens pirilampo* is distinguished from all congeners, except *A. plagiozonatus*, by having anteriorly oblique dark brown flank bars (*vs.* vertical). The new species differs from *A. plagiozonatus* by having the dorsal head contour, from the tip of the snout to the vertical through the posterior margin of the eye, almost straight, except for a conspicuous concavity at the interorbital region (Fig. 2) (*vs.* dorsal head contour convex, with a subtle concavity at the interorbital region in occasional specimens), by having longer lower jaw (40.2–46.9% HL and 16.7–18.5% SL *vs.* 35.2–39.3% HL and 13.2–15.2% SL in *A. plagiozonatus*), and longer upper jaw, (12.2–15.1% SL *vs.* 9.3–12.1% SL in *A. plagiozonatus*). Additionally, *A. pirilampo* is distinguished from its congeners, except *A. chimantanus* Inger, 1956, *A. diadema*, *A. epae*, *A. mauesanus* Kullander, 1997, *A. michaeli*, *A. patricki* Kullander, 1984, *A. plagiozonatus*, *A. potaroensis* Eigenmann, 1912, and *A. tubicen* Kullander & Ferreira, 1991, by having a discontinuous lateral band in fixed specimens (*vs.* continuous). *Aequidens pirilampo* differs from *A. diadema* and *A. epae* by having the lateral band divided into blotches more conspicuous at the encounter with flank bars (*vs.* lateral band not divided into blotches), and by the absence of unpigmented areas anteriorly and posteriorly to the midlateral spot, not forming a whitish circle above the longitudinal stripe (*vs.* presence). *Aequidens pirilampo*, also differs from *A. epae* by having the dorsal portion of the flank bar 5 anteriorly inclined and less conspicuous than the midlateral spot (*vs.* posteriorly inclined and as dark as the midlateral spot). *Aequidens pirilampo* also differs from *A. rondoni* (Miranda Ribeiro, 1918) by having eight flank bars (1a, 1p, 2, 3, 4, 5, 6, and 7; Fig. 4) instead of nine (1a, 1p, 2 bars, 3–4 expressed as three bars, 5, 6, and 7). *Aequidens pirilampo* differs from *A. mauseanus*, *A. michaeli* and *A. potaroensis* by having the lateral band equally conspicuous along its entire length (*vs.* lateral band more inconspicuous anterior to midlateral spot in *A. mauseanus* and *A. potaroensis*, and posterior to midlateral spot in *A. michaeli*); from *A. mauseanus* by the absence of a dark-brown blotch dorsal to midlateral spot (*vs.* presence); from *A. michaeli* by having a cheek spot (*vs.* absence), and by the absence of iridescent vermiculations on the cheek, opercle and pectoral girdle (*vs.* more ornamented pattern with stripes present in the cheek, opercle and pectoral girdle); from *A. paloemeuensis* Kullander & Nijssen, 1989 and *A. potaroensis* by the suborbital stripe not retained in adult specimens (*vs.* retained). *Aequidens pirilampo* differs from *A. patricki* by the absence of large, dark-brown blotches on the cheek and opercle (*vs.* presence), and by the brown

lachrymal region (*vs.* unpigmented). *Aequidens pirilampo* differs from *A. tubicen* by the absence of a preopercular spot (*vs.* presence). Additionally, *Aequidens pirilampo* differs from *A. gerciliae* by the round midlateral spot (*vs.* longitudinally elongated); from *A. metae* Eigenmann, 1922 by the cheek spot not spanning the entire anterior margin of the vertical arm of the preopercle (*vs.* spanning the entire anterior margin of the vertical arm of the preopercle); from *A. superomaculatum* Hernández-Acevedo, Machado-Allison & Lasso, 2015 by the absence of a posterodorsal blotch on the flank (*vs.* presence).

Description. Based on holotype and paratypes. Measurements in Tab. 1. See also Figs. 2–4 for details of shape and color pattern. Body laterally compressed. Predorsal contour ascending straight from tip of snout to vertical through posterior margin of orbit. Moderately convex from this point to end of dorsal fin; straight along caudal peduncle. Prepelvic contour descending straight or slightly convex from tip of snout to vertical through posterior margin of preopercle, at same angle of predorsal contour (young specimens have more obtusely angled predorsal contour than prepelvic). Abdominal contour straight or slightly convex and horizontal. Anal-fin base contours straight and oblique. Caudal peduncle ventral contour straight or slightly concave and horizontal.

Head elongate, triangular in lateral view, with dorsal margin, from tip of snout to end of supraoccipital, ascending straight and oblique, ventral contour less steep than dorsal contour. Groove between eyes. Snout long, with frontal contour elongated and continuous with dorsal and ventral contour of head. Lips thick and of "American type", *i.e.*, lower lip fold covers upper lip. Tip of maxilla almost reaching vertical through anterior margin of eye. Nostril dorsolaterally situated, below horizontal through lower margin of orbit, halfway between tip of snout and orbit (in young specimens, closer to eye, horizontal through middle of eye). Orbit large, situated on dorsal half of head, pupil ventral to level of upper lateral line. Posterior margin of preopercle, opercle, subopercle, interopercle and suprachleitrum smooth, without serrations.

E1 scales 24(18), 25*(14) or 26(1). Scales between upper lateral line and dorsal-fin 3* (24), 3½ (9) at base of first dorsal-fin spine, 1½(27), 2*(5), 2½(2) at base of last dorsal-fin spine. Scale rows between lateral line 2*(27). Scales on lateral line 13/8(1), 14/8(1), 15/7(2), 15/8(2), 16/6*(2), 16/7(5), 16/8(5), 17/6(1), 17/7(2), 17/8(5); additionally 1(4), 2*(23) or rarely 3(1) scales of lower lateral line onto caudal fin. Cheek scales in 3*(9), 3½(10), or 4(10) rows, ctenoid. Opercle scales 4(1), 5(2) or 6*(23), large and cycloid, stochastically arranged. Subopercle covered with 3*(32) cycloid scales. Interopercle with 2(15), 3*(14) or 4(2) scales embedded in skin. Scales absent from preopercle. Infraorbital scales 5(3), 6*(25) or 7(4). Circumpeduncular scale rows 16*(35), including lateral line scales. Predorsal scales uniserial(2), biserisal(2), triserial*(24) or stochastic(1), cycloid, slightly smaller than flank scales. Flank scales ctenoid. Prepelvic scales 6(1), 7(3), 8(4), 9(1), 10*(12), 11(7), 13(1), ctenoid, same size towards gular region. Abdominal scales ctenoid, slightly smaller than flank scales. Pectoral, pelvic, dorsal, and anal fins without scales. Caudal-fin base covered with stochastically distributed transition scales, intermediate in size between peduncular and inter-radial scales; caudal fin with cycloid inter-radial scales from base of rays to ⅓ of its length; series increasing ontogenetically, 2–5 scales in specimens up to 40 mm covering from basal ⅛ to basal ⅙, 4–14 scales in specimens over than 40 mm SL, covering from basal ¼ to basal ⅓, without secondary series; one specimen (NUP 21644, 68.5 mm SL) with series of scales with pores and canals between rays D3–D4 (8 scales) and V3–V4 (8 scales).

TABLE 1 | Morphometric data of *Aequidens pirilampo*. N = total number of specimens examined; SD = Standard deviation.

	Holotype	Paratypes			
		N	Range	Mean	SD
Standard length (mm)	94.7	26	40.1–94.0	60.0	–
Percents of standard length					
Body depth	43.7	26	41.9–46.6	44.2	1.4
Preanal distance	74.1	26	72.8–79.4	76.4	1.6
Prepelvic distance	45.5	26	43.9–48.5	46.4	1.1
Prepectoral distance	39.9	26	37.7–44.4	41.3	1.6
Predorsal distance	43.4	26	42.6–48.8	46.0	1.7
Distance from dorsal to caudal fin	70.2	26	63.9–68.8	66.2	1.2
Distance from dorsal to anal fin	56.6	26	52.9–57.6	55.5	1.2
Distance from dorsal to pelvic fin	42.8	26	42.2–46.6	43.9	1.2
Distance from dorsal to pectoral fin	26.5	26	26.5–31.4	28.4	1.2
Caudal peduncle depth	16.9	26	15.5–17.6	16.7	0.5
Caudal peduncle length (straight)	7.7	26	4.9–8.0	6.0	0.7
Caudal peduncle length (oblique)	12.0	26	10.2–12.3	11.0	0.5
Pectoral-fin length	30.6	25	28.5–33.6	31.0	1.4
Pelvic-fin length	32.8	26	28.1–39.6	32.2	2.7
Pelvic spine length	12.2	26	11.9–15.7	13.5	1.0
Dorsal-fin base length (spine)	42.1	26	40.3–46.9	42.8	1.6
Dorsal-fin base length (total)	61.3	26	54.6–61.4	58.6	1.6
Last dorsal-fin spine length	11.8	26	11.5–15.1	13.0	1.0
Anal-fin base length (spine)	5.2	26	4.2–6.5	5.3	0.5
Anal-fin base length (total)	19.5	26	16.7–19.6	18.2	0.8
Last anal-fin spine length	12.9	26	11.4–15.6	12.9	0.9
Head length	39.1	26	37.8–43.0	40.5	1.3
Head depth	38.9	26	34.7–39.9	37.1	1.7
Head width	18.7	26	17.6–20.9	19.3	0.9
Orbital diameter	9.0	26	10.5–15.0	12.7	1.3
Postorbital head length	14.9	26	14.4–15.5	14.9	0.3
Interorbital distance	13.1	26	9.2–19.2	11.0	1.8
Snout length	15.7	26	11.6–15.2	13.7	0.9
Cheek depth	11.0	26	8.7–11.8	10.5	0.8
Lachrymal depth	8.2	26	5.0–7.8	6.7	0.8
Upper jaw length	14.2	26	12.2–15.1	13.6	0.8
Lower jaw length	17.5	26	16.8–19.2	17.9	0.6
Midlateral spot length	9.4	26	7.9–10.7	9.5	0.7
Percents of head length					
Head depth	99.5	26	69.8–100.5	91.5	4.8
Head width	47.8	26	45.2–51.1	47.6	1.7
Orbital width	23.0	26	23.0–36.5	31.4	2.6
Postorbital	38.1	26	35.3–39.2	36.8	0.9
Interorbital width	33.4	26	23.0–46.6	27.2	4.5
Snout length	40.2	26	24.9–40.2	33.7	2.2
Cheek depth	28.2	26	21.4–31.1	25.9	2.3
Lacrimal depth	20.9	26	12.4–20.9	16.5	2.3
Upper jaw length	36.3	26	29.7–38.0	33.6	2.3
Lower jaw length	44.7	26	40.2–46.9	44.1	1.6

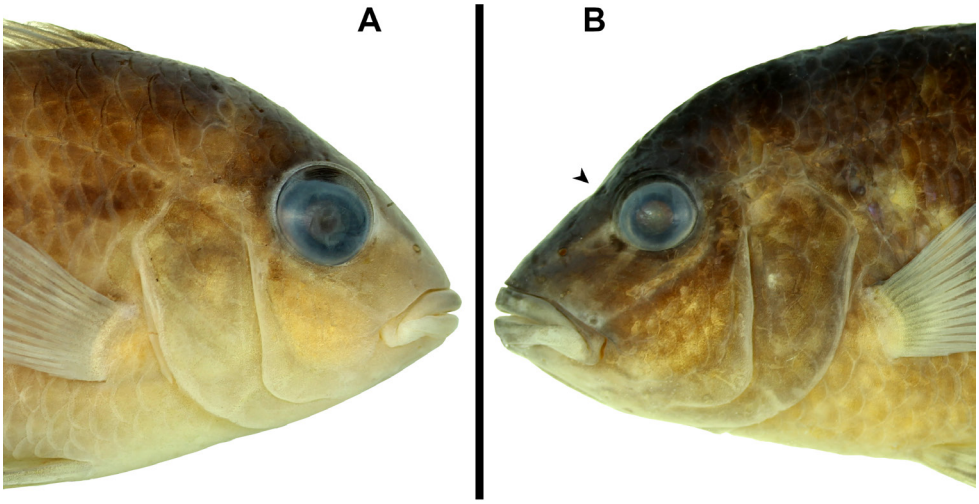

FIGURE 2 | Head profile (**A**) convex in *Aequidens plagiozonatus*, NUP 13372, 76.6 mm SL, horizontally inverted, and (**B**) triangular in *A. pirilampo*, NUP 23543, 94.7 mm SL holotype. Arrow indicates the groove between the eyes.

FIGURE 3 | *Aequidens pirilampo*, living specimens photographed just after capture in the rio Comprido, rio Paraguai River basin, 17°32'04.8"S 54°25'36.6"W, uncatalogued. Photos by L. F. C. Tencatt.

Dorsal-fin rays XIV.10(1), XIV.11(3), XV.9(2), XV.10(19), XV.11*(7); dorsal spines increasing in size up to 6th, first spine about one-fourth length of last. Dorsal-fin rays 4–5 forming filament reaching over ⅔ of caudal fin length in some specimens; lappets rounded to pointed, with posterior margin free, slightly surpassing tip of spines. Anal-fin rays III.7.i(3), III.8(4), III.8.i(19), III.8.ii(2), III.9*(4) or IV.9(1); middle rays longest, pointed, in some specimens forming filament reaching up to half of caudal-fin length. Caudal-fin rounded, with 14*(32) principal rays. Total pectoral-fin rays 12(2), 13(13), 14*(18) or 15(1). Pectoral fin ventrally rounded, dorsally pointed, fourth ray longest, in some specimens passing posterior margin of midlateral spot. Pelvic-fin rays I.5*(34); second ray longest, with filamentous extension, reaching or passing anal-fin origin.

Gill rakers externally on first epibranchial 1(10) or 2*(24); 0(2) or 1*(32) on angle; 4(8), 5*(20), 6(3) or 7(1) on ceratobranchial 1.

Teeth unicuspid, decreasing gradually from symphysis. Symphysis of both jaws lacking teeth. Upper jaw series with 3–4 rows; lower jaw series with 2–4 rows. External hemiseries of upper jaw right/left sides with 9–13/11–12 in specimens up to 40 mm; 10–22/6–23 in specimens over 40 mm. External hemiseries of lower jaw right/left sides with 16–21/17–21 in specimens up to 40 mm; 17–25/11–26 in specimens over 40 mm.

Suture between contralateral ceratobranchial 5 not including interdigitations ventrally; posteromedial teeth large, cylindrical, with large, blunt, dorsally oriented cusp and 1–2 very small, anteriorly oriented cusps; anterolaterally, teeth gradually diminishing in size; outer teeth compressed transversally, with large cusp and 1–2 very small, upward cusps. Lower pharyngeal jaw tooth-plate (ceratobranchial 5) (Fig. 5) length including posterolateral processes 89.9% of width; length of dentigerous area 59.8% of width; 13 teeth along posterior margin each side; seven teeth along symphyseal margin; 22 teeth along outer margin. Pharyngobranchial 2 with seven teeth arranged in two rows, posteriormost ones larger, turned anteriad. Pharyngobranchial 3 with 34 teeth arranged in 6 rows turned backwards. Tooth plate 4 with 51 teeth arranged in 7 rows turned posteriad; three concavities in the frayed zone at the posterior margin. Ceratobranchial 4 with 2 tooth plates, posterior with 5–6 teeth, anterior with 6–9 teeth. Two supraneurals, anterior to first neural spine. Twenty-seven total vertebrae, of which 13(2) abdominal (4 and 5 type A', others type A) and 13(2) caudal (first 12 type and PU1+U1). Three posteriormost vertebrae (CV3, CV2 and PU1+U1) completely included in the caudal peduncle. Ribs 10, abdominal. Vertebrae bearing ribs, 3rd–12th. Epineurals absent. Twenty-four dorsal-fin pterygiophores (one spine or ray for each pterygiophore), surrounded by vertebrae 1–20. Ten anal-fin proximal pterygiophores (first one bearing first two spines; last one bearing last two rays), surrounded by vertebrae 13–20 (anteriormost pterygiophore touches the anterior margin of haemal spine of 14th vertebra). Two epurals. One uroneural. Five branchiostegal rays. First branchial arch with 7 outer rakers (one on epibranchial, one on angle, and five on ceratobranchial) and 11 inner rakers (2 on epibranchial, one on angle, and 8 on ceratobranchial). Second arch with 12 external rakers (two on epibranchial, one between epibranchial and ceratobranchial, eight on ceratobranchial, and one between ceratobranchial and hypobranchial) and 8 inner rakers (on ceratobranchial). Third arch with 11 external rakers (one on epibranchial, one between epibranchial and ceratobranchial, and nine on ceratobranchial) and 11 inner rakers (one on epibranchial, two between epibranchial and ceratobranchial, and eight on ceratobranchial). Fourth arch with 11 external rakers

(one on epibranchial one between epibranchial and ceratobranchial, and nine on ceratobranchial) and 10 inner rakers (epibranchial lacking rakers, all on ceratobranchial). Two procurrent caudal-fin rays dorsally and three ventrally. Microbranchiospines on all four branchial arches.

Coloration in alcohol. Background light beige to yellowish brown; ventral region yellowish white; dorsal region dark brown. Posterior margin of flank scales with diffuse brown pigmentation. Head brownish on neurocranial region and nape; yellowish-brown on cheek, preopercle and opercle region; and yellowish white ventrally. Cheek spot dark brown. Three oblique, beige stripes continuous across dorsal midline of head. First along anterodorsal margin of lachrymal, from tip of snout to anterior margin of orbit, through nostril. Second from near anteroventral margin of lachrymal to anteroventral margin of orbit. Third along posteroventral margin of lachrymal and infraorbitals. Stripes absent from cheek, gill cover and pectoral girdle. Nine bars along body being eight bars on flank and one (bar 9) on head (Figs. 4A, B): bar 1p, at caudal-fin base, forming blotch; bar 1a, on distal portion of caudal peduncle; bar 2, at vertical through last soft dorsal- and anal-fin rays; bar 3, at vertical through first soft dorsal- and anal-fin rays; bar 4, at vertical through last dorsal-fin spine and anal-fin spines; bar 5, usually at vertical through 8th–11th dorsal-fin spines and vent; bar 6, usually at vertical through 4th–8th dorsal-fin spines and posterior to pelvic-fin base; bar 7, usually at vertical through base of first dorsal-fin spines to pectoral-fin origin; bar 8, on nape and, more diffusely, on opercle; bar 9, formed by supraorbital and infraorbital bars, the latter present only in young specimens (Figs. 4C–F). Lateral band dark brown, divided into blotches at intersections with flank bars, mainly concentrated along E1 scale series. Midlateral spot on bar 5, covering E1 and E2 series. Beige to brown fins. Dorsal fin lighter on distal margin; small, rounded white blotches on soft portion, in occasional specimens forming oblique stripes. Anal fin with same pattern as dorsal fin. Caudal fin lighter on distal margin; small white blotches more concentrated on anterior two thirds, forming dotted or striped pattern (better viewed in fixed and smaller specimens) (Fig. 4); one black blotch, usually ocellated, corresponding to bar 1p, at base of all rays of dorsal lobe.

Coloration in life. Based on Fig. 3 and field observations by LFCT (2018–2021). Background pale to light beige; ventral region whitish. Head brownish in dorsal region, with silvery scales on nape; lachrymal and cheek silvery, border of the scales yellow to brownish, with black cheek spot posteroventral to orbit, between third oblique stripe below lacrimal and preopercle upper portion; preopercle and interopercle silvery, subopercle light beige; opercle light brownish, border of the scales yellow to silvery brownish; middorsal portion typically with brownish orange patch; ventral region light beige. Body covered by green, yellow, and blue iridescent coloration. Scales on flank silvery, forming a more evident reticulated pattern, with brownish borders at posterior margin. Pattern of dark blotches, stripes, and bars less evident than in preserved specimens, but similar in relation to number and position of color-pattern elements. Fins yellowish. Dorsal fin with white blotches at membranous region between spines/rays, with distal portion yellow. Anal fin with distal portion yellow, blotches as same pattern as preserved specimens. Pelvic fin yellowish at first spine and rays region, proximal region light beige, distal region yellowish. Caudal fin yellowish, base with blue iridescent spots/stripes.

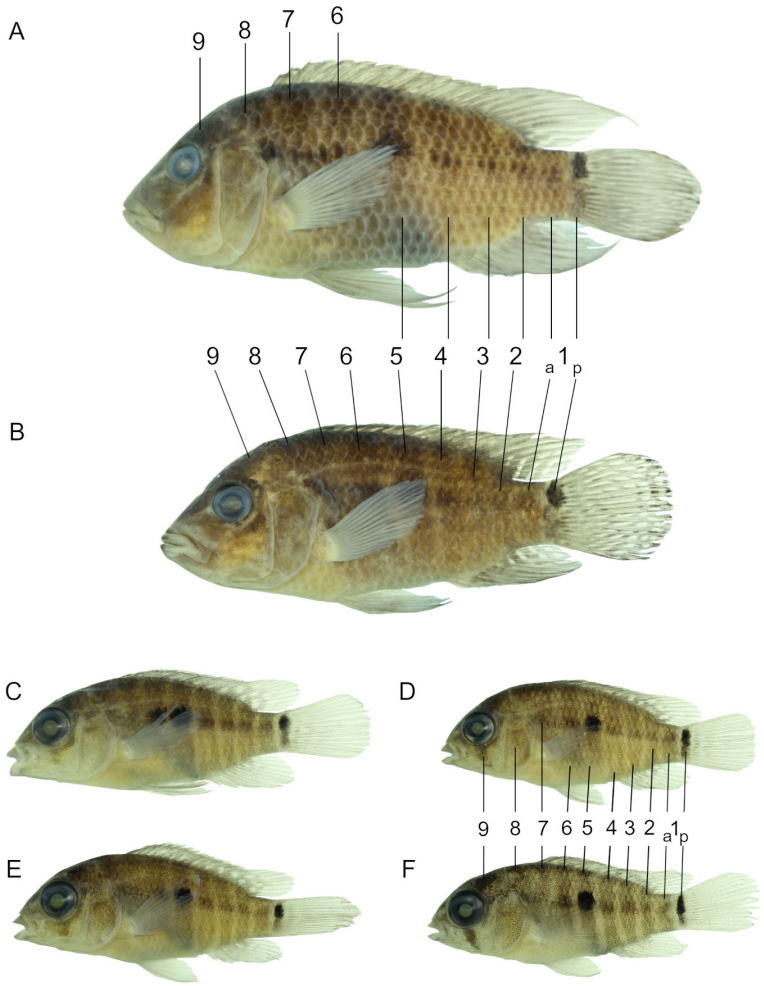

FIGURE 4 | Coloration and ontogenetic variation in *Aequidens pirilampo*, NUP 23544, (**A**) 87.2 mm SL, (**B**) 65.7 mm SL, (**C**) 24.6 mm SL, (**D**) 22.8 mm SL, (**E**) 22.5 mm SL, and (**F**) 14.6 mm SL, collected with holotype. Bar 9 includes the infraorbital bar in smaller specimens (**C**-**F**).

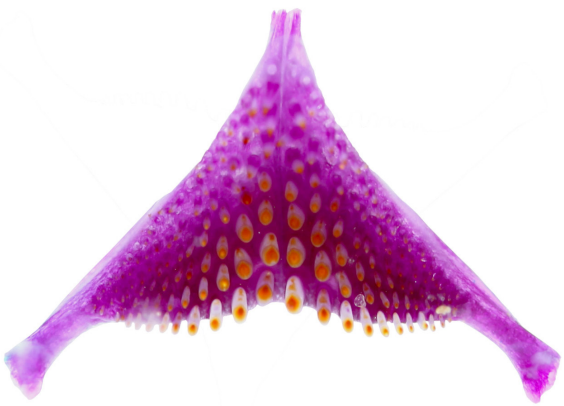

FIGURE 5 | Ceratobranchials 5 (lower pharyngeal jaw) of *Aequidens pirilampo*, NUP 23547, paratype, 59.2 mm SL, in the occlusal plane, with anterior portion upwards.

Geographical distribution. *Aequidens pirilampo* is currently only known from tributaries of the upper rio Correntes, a tributary of the rio Paraguai basin, in the border region between Mato Grosso and Mato Grosso do Sul states, Brazil (Fig. 6).

Ecological notes. General view on the collecting sites of *Aequidens pirilampo* in Fig. 7. The new species lives in lentic mesohabitats with depths ranging from around 10 cm (particularly hatchlings) to slightly over 1 m with a lot of submerged vegetation (macrophytes in general, including those floating in some points). Unlike other *Aequidens* species, which are usually found in brownish water (tea-colored water) environments, the upper rio Correntes and its tributaries present extremely crystalline water except for environments degraded by anthropic impacts, allowing the observation of solitary fish foraging close to submerged vegetation during the day. The species is found in syntopy with *Astyanax* sp., *Characidium chicoi*, *Characidium* aff. *zebra* Eigenmann, 1909, *Cnesterodon* cf. *septentrionalis* Rosa & Costa, 1993, *Cyphocharax caboclo*, *Eigenmannia correntes*, *Hyphessobrycon* sp., *Hypostomus* sp., *Melanorivulus* cf. *dapazi* (Costa, 2005), and *Moenkhausia lopesi* Britski & Silimon, 2001. The subterranean stretch (or the sinkhole itself) of the rio Correntes is hypothesized to be a barrier to the fish fauna of the basin. However, *Aequidens pirilampo*, as well as the other four endemic species described from the upper rio Correntes basin, were not found in all sampling sites upstream the sinkhole during the four years of survey efforts in the region. In the Ponte de Pedra hydroelectric

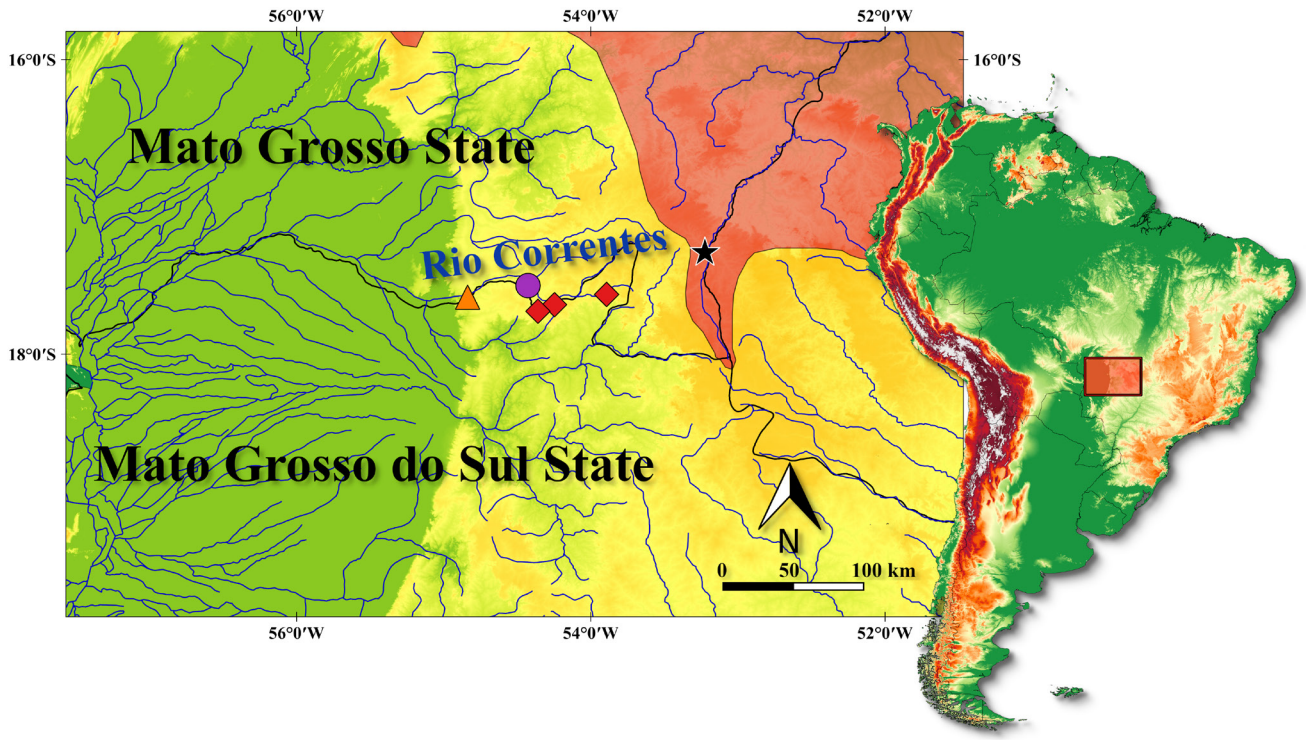

FIGURE 6 | Partial map of South America showing the distribution of *Aequidens pirilampo*, in the rio Paraguai basin (yellow shade), Brazil. Purple circle, type-locality in the córrego Comprido, rio Correntes basin; red diamonds, additional localities, rio Correntes basin; orange triangle, sinkhole; black star, locality of *A. plagiozonatus* in the rio Boiadeiro, rio Araguaia basin (red shade).

FIGURE 7 | Collecting sites of *Aequidens pirilampo*, showing (**A**) the ribeirão Comprido, its type-locality, (**B**) a stream with unknown name, and (**C**) the córrego de Cima, all tributaries of the rio Correntes in the border region of Mato Grosso and Mato Grosso do Sul states, Central Brazil. Photo (**A**) by LFCT, (**B**) by Heriberto Gimênes Jr., and (**C**) by Hans Evers.

power station Reservoir (just upstream of the sinkhole), none of these endemic species was captured. At this site, only *A. plagiozonatus* was found (Fig. 8A), along with several other species common to most tributaries of the upper rio Paraguai basin (*e.g.*, *Saxatilia lepidota* (Heckel, 1840), *Hyphessobrycon herbertaxelrodi* Géry, 1961, *Megalechis thoracata* (Valenciennes, 1840), *Metynnis* cf. *maculatus* (Kner, 1858), and *Satanoperca pappaterra* (Heckel, 1840), including some introduced species like *Cichla* spp. and *Colossoma* sp. (the last one not captured, with occurrence confirmed by several locals). Considering the currently available data, it seems that a large waterfall (estimated to be at least 50 m high; 17°32'06"S 54°26'01"W) in the area of a small hydroelectric power plant represents the downstream limit of occurrence of the new species. *Aequidens pirilampo* is the only cichlid known to occur upstream at this point. None of the aforementioned species, except for the new species, was captured upstream of this waterfall.

Etymology. The specific epithet "*pirilampo*" means firefly in the popular Portuguese naming in the region the new species occurs. It is a bioluminescent Coleoptera very common in this region. These insects emit an intense green light, which alludes to the color pattern in life displayed by the new species. A noun in apposition.

FIGURE 8 | General morphology and color pattern of *Aequidens plagiozonatus* of (**A**) an uncatalogued specimen captured in the Ponte de Pedra Reservoir, rio Correntes, rio Paraguai basin, a couple of days after preservation, and (**B**) an uncatalogued living specimen captured in the rio Boiadeiro/córrego Gordura, rio Araguaia basin, both specimens with about 70.0 mm SL. Photo (**A**) by LFCT and (**B**) by Hans Evers.

Conservation status. The new species is currently known from two tributaries of the upper rio Correntes basin, which is severely impacted due to intense agricultural activity (see Melo *et al*., 2022) causing a decrease in riparian plant cover and, as a result, a silting process. Additionally, the region has been impacted by the installation of hydroelectric power plants, and further hydroelectric projects are already planned (see ANA, 2019). The Extent of Occurrence (EOO) of *Aequidens pirilampo* was estimated at about 200 km^2. Therefore, considering the relatively restricted geographic distribution of the new species and the severe anthropic impacts in the region, and according to the International Union for Conservation of Nature (IUCN) categories and criteria (IUCN, 2022), *Aequidens pirilampo* is herein suggested to be classified as Near Threatened (NT), approximating the Endangered (EN) category by criterion B1b(iii).

Common name. *Aequidens pirilampo* is popularly known as 'cará'.

Molecular analysis. The final matrix of *Aequidens* species comprises 25 terminal taxa (including 23 species of *Aequidens*) and 402 characters, being 303 conserved and 99 variable sites (of which 96 were parsimony-informative), with 22.8% adenine, 28.7% cytosine, 31.7% thymine and 16.8% guanine (% in relation to the entire alignment).

The estimated index of substitution saturation (Iss) performed in DAMBE 5.2.31 (Xia, Xie, 2001) showed that the data was not saturated (*i.e*., Iss.c value greater than Iss). Genetic distances (Kimura, 1980) of the COI gene between *Aequidens pirilampo* and other *Aequidens* and *Cichlasoma* species are presented in Tab. 2. All species delimitation analyses corroborate the separation of *A. pirilampo* from the other *Aequidens* and *Cichlasoma* species included in this study (Fig. 9).

TABLE 2 | Interspecific Kimura 2-parameter mean distance of *Aequidens* and *Cichlasoma* species (below diagonal) and standard errors (above diagonal) were obtained by a bootstrap procedure.

	Species	1	2	3	4	5	6	7	8	9	10	11	12	13
1	*Aequidens pirilampo*		0.0096	0.0246	0.0215	0.0157	0.0156	0.0235	0.0227	0.0287	0.0213	0.0195	0.0218	0.0238
2	*Aequide plagiozonatus*	0.0307		0.0257	0.0213	0.0156	0.0155	0.0230	0.0214	0.0286	0.0211	0.0195	0.0219	0.0228
3	*Aequidens diadema*	0.1752	0.1861		0.0198	0.0218	0.0231	0.0082	0.0208	0.0314	0.0235	0.0239	0.0222	0.0256
4	*Aequidens gerciliae*	0.1480	0.1477	0.1274		0.0210	0.0217	0.0182	0.0112	0.0274	0.0200	0.0191	0.0199	0.0218
5	*Aequidens tetramerus*	0.0892	0.0890	0.1552	0.1465		0.0072	0.0204	0.0191	0.0265	0.0194	0.0182	0.0209	0.0206
6	*Aequidens epae*	0.0857	0.0855	0.1621	0.1483	0.0242		0.0214	0.0201	0.0271	0.0206	0.0194	0.0215	0.0214
7	*Aequidens pallidus*	0.1744	0.1714	0.0407	0.1216	0.1498	0.1532		0.0189	0.0269	0.0218	0.0216	0.0208	0.0239
8	*Aequidens michaeli*	0.1644	0.1575	0.1433	0.0467	0.1322	0.1355	0.1358		0.0261	0.0185	0.0181	0.0211	0.0206
9	*Pterophyllum altum* (outgroup)	0.2383	0.2350	0.2653	0.2263	0.2181	0.2239	0.2271	0.2119		0.0276	0.0275	0.0281	0.0289
10	*Cichlasoma paranaense*	0.1530	0.1493	0.1710	0.1328	0.1286	0.1364	0.1652	0.1214	0.2300		0.0079	0.0169	0.0192
11	*Cichlasoma dimerus*	0.1340	0.1305	0.1739	0.1235	0.1164	0.1242	0.1590	0.1173	0.2275	0.0264		0.0181	0.0186
12	*Cichlasoma sanctifranciscense*	0.1567	0.1597	0.1581	0.1344	0.1439	0.1466	0.1553	0.1489	0.2254	0.1038	0.1140		0.0192
13	*Cichlasoma orientale*	0.1845	0.1702	0.2023	0.1591	0.1491	0.1568	0.1935	0.1493	0.2348	0.1280	0.1206	0.1206	

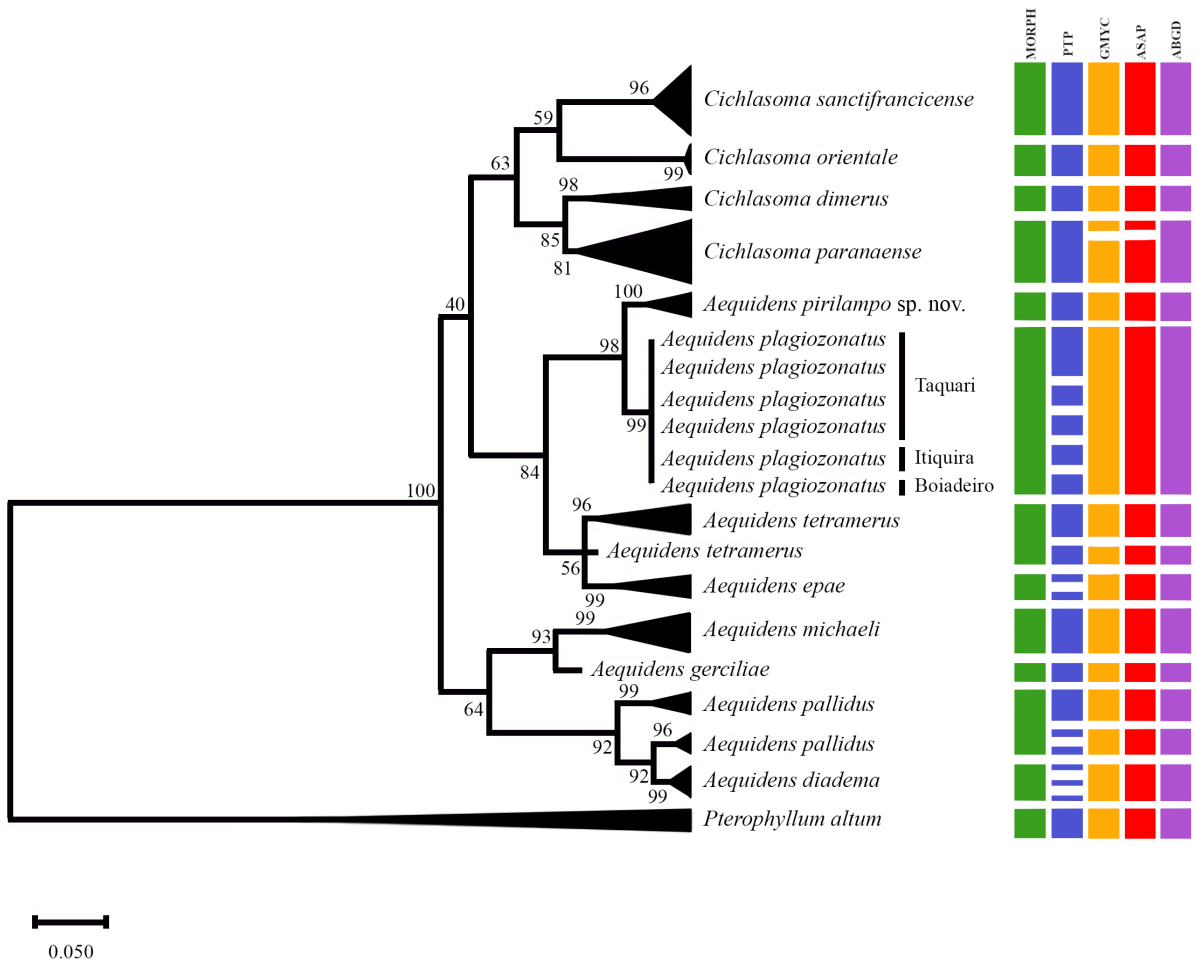

FIGURE 9 | Maximum-likelihood tree based on the cytochrome oxidase c subunit I gene (COI) partial sequence and the species delimitation analyses evidencing the *Aequidens pirilampo*, clade (rio Paraguai basin) and the presence of *A. plagiozonatus* in the rio Paraguai (rios Taquari and Itiquira), and rio Araguaia basin (rio Boiadeiro). Morph.: morphological analysis. Notes labeled with numbers represent bootstrap support.

The ML tree inferred through MEGA-X recovered the two groups consistent with the genetic distance analysis and the previous morphological identification of species and exhibited strong node support for each species, *i.e.*, 100% for the *A. pirilampo* clade and 99% for *A. plagiozonatus* clade (Fig. 9) (see Figs. **S2, S3, S4, S5**) for details in the delimitation analyses). The ABGD analysis resulted in eight partitions that ranged from 96 (P = 0.036) to 169 (P = 0.00113) lineages, with three partitions (P = 0.0031–0.00821) resulting in 15 lineages, and the ASAP analysis resulted in 10 partitions that ranged from 7 (score = 5.5) to 21 (10.5) lineages, with one partition with 16 lineages (lowest score = 3.0) (Fig. 9). All species delimitation analyses support the presence of two species of *Aequidens* occurring in the rio Paraguai basin, the first, *A. pirilampo*, described herein, and the second, *A. plagiozonatus* occurring in both the rio Paraguai and Araguaia basins, however, PTP analysis recovered several lineages within *A. plagiozonatus*.

Material comparative examined. Brazil, rio Amazonas basin: *Aequidens gerciliae*: NUP 7200, 3, 52.7–59.1 mm SL. NUP 7483, 1, 46.7 mm SL. NUP 18442, 1, 82.4 mm SL. *Aequidens pallidus*: NUP 17281, 83.0 mm SL. *Aequidens tetramerus*: INPA 972, 84.7 mm SL. NUP 17983, 6, 34.9–140.9 mm SL. NUP 19382, 1, 76.9 mm SL. **Rio Araguaia basin:** *Aequidens plagiozonatus*: LBP 30741, 1, 39.2 mm SL. **Rio Paraguai basin:** *Aequidens plagiozonatus*: LBP 1912, 5, 43.9–61.8 mm SL. LBP, 1925, 3, 40.7–54.0 mm SL. LBP 10767, 3, 41.1–56.7 mm SL. NUP 194, 3, 77.0–88.8 mm SL. NUP 13372, 3 (2 c&s), 57.1–76.6 mm SL. NUP 21604, 3, 37.4–52.0 mm SL. NUP 21621, 3, 25.4–48.2 mm SL. NUP 21368, 1, 81.4 mm SL. **Rio Tapajós basin:** *Aequidens rondoni*: MNRJ 1616, photograph and x-ray of the holotype of *Acaropsis rondoni*. **Guyana, rio Potaro:** *Aequidens potaroensis*: FMNH 53892, photograph of the holotype, 140 mm SL. **Venezuela, rio Orinoco basin:** *Aequidens chimantanus*: FMNH 45702, photograph of the holotype.

DISCUSSION

The generic allocation of *Aequidens pirilampo* in *Aequidens* as opposed to *Cichlasoma* is supported by the scaleless dorsal and anal fins (scaled in *Cichlasoma*), a longer caudal peduncle with 2–3 vertebrae (2 or 0 in *Cichlasoma*), and 4–5 vertical bars from the midlateral spot to the caudal peduncle in *Aequidens* (6 in *Cichlasoma*) (Kullander, 1986). Our results from the molecular analysis support previous hypotheses in which *Cichlasoma* is nested together with *Aequidens* (Musilová *et al*., 2008; Ilves *et al*., 2018).

Herein, morphological and molecular analyses support the species delimitation of *Aequidens pirilampo*. The only other valid species of *Aequidens* described from the rio Paraguai basin is *A. plagiozonatus* (Fig. 8), which shares with *A. pirilampo*, the obliquely oriented flank bars, but in the new species this pattern is less conspicuous. Unlike *A. plagiozonatus*, the caudal fin of some individuals of *A. pirilampo*, has a dotted or striped pattern, more conspicuous in fixed and smaller to medium specimens. The only other species with anteriorly inclined flank bars is *A. viridis* (see Kullander, 1984). However, in *A. viridis* only bars 6 and 7 are inclined, while in *A. pirilampo*, bars 3 through 7 are inclined. Furthermore, the head profile in lateral view is very triangular in *A. pirilampo*, instead as rounded as in *A. viridis* and *A. plagiozonatus*.

Characters previously used to group species of *Aequidens* are not well-defined. For example, buccal stripes and counts in vertebrae were used to classify species in unnamed artificial groupings (Kullander, 1995). Here, *A. pirilampo* has 13+13 vertebrae count, with only a distinction in the fourth and fifth abdominal vertebrae presenting short, paired hypapophyses, but co-ossified (see character 77 in Kullander, 1998). However, as Kullander (1995) identified the usual 13+13 vertebrae count in *A. epae*, *A. gerciliae*, and *A. michaeli* (the latter occasionally with 25, 26 or 27), being traits not exclusive. The new species is more closely related to *A. plagiozonatus* in the ML approach, and does not fit in any previously defined artificial species group of *Aequidens*.

Říčan *et al.* (2005) investigated the evolution and development of the melanophoric coloration in Neotropical cichlids and observed that the homology between individual marks is better understood when ontogenetic series are available for interspecific comparisons. They concluded that, in *Cichlasoma*, flank bar 4 splits during development, giving place to bar 4a and bar 4p (Říčan *et al*., 2005, figs. 33–36). By contrast, in species of *Aequidens* the flank bar 4 usually does not split during ontogeny (Říčan *et al*., 2005, figs. 26, 28), albeit some specimens of *Aequidens* may present a split flank bar 4 (see Kullander,

1995, fig. 17, for an example of *Aequidens michaeli*). Furthermore, in some species of *Aquidens*, such as *A. diadema*, *A. mauseanus*, *A. metae*, *A. pallidus*, *A. superomaculatum*, the flank bars 2 and 3 appear to be fused, similarly to the pattern in *Satanoperca setepele* Ota, Deprá, Kullander, Graça & Pavanelli, 2022. Therefore, the increased number of bars in *Cichlasoma* represents a division of the same bar by melanophore migration through ontogeny.

The ventral portion of bar 9 forms the suborbital stripe and is present in the young of all *Aequidens* species. This pattern is retained in adults only in *A. paloemeuensis* and *A. potaroensis* according to original descriptions and Kullander (2012), but lost in the other species. These two species were found to belong to the genus *Krobia* (*K. potaroensis*, *K. paloemeuensis*) by Musilová *et al*. (2009). However, according to morphological characters, both species pertain to *Aequidens* (see discussion section in Kullander, 2012). Due to a lack of larval material, we were unable to identify the development of the bars via the union of melanophore patches as described by Ota *et al*. (2021) and Deprá *et al*. (2022). A cheek spot is located between the posteroventral margin of the eye and the vertical arm of the preopercle, and is more evident in adults than in the young.

Integrative analyses have been performed as a useful tool to support species delimitations and to confirm species assignments (Padial *et al*., 2010; Gomes *et al*., 2015; Dellicour, Flot, 2018; Garavello *et al*., 2021), as well as to access phylogenetic relationships among the different species.

Herein, the validity of *Aequidens pirilampo* is investigated through phenotypical exam and several analyses using molecular data. The ML tree based on *mt-co1* sequences recovers *A. pirilampo* and *A. plagiozonatus* as sister species. The analysis of barcoding indicates interspecific genetic divergence more than 2%, which is considered a suitable threshold for species delimitation (Carvalho *et al*., 2011; Pereira *et al*., 2011a,b, 2013) including for some cichlid species (Souza *et al*., 2018). Depending on the group studied, the interspecific genetic divergence can be found lower than 2% and this cutoff value is only a start point based on the distribution of K2P values of species barcoded available in BOLD system showing that evolutionary history should be considered (http://www.boldsystems.org, and see discussion in Pereira *et al*., 2013). But an operational taxonomic unit (OTU) has most likely been retrieved when more than 50% of the species delimitation techniques agree (Ramirez *et al*., 2023).

The Central Brazil, constituted by the rio Amazon-Paraguai-Araguaia basins, is known to have fish species interchange, as evidenced by some events as headwater-capture (*i.e*., adjacent basins capturing ichthyofauna from each other) (Aquino, Colli, 2017; Dagosta, de Pinna, 2017; Machado *et al*., 2018; specifically for the studied area Melo *et al*., 2022). *Aequidens plagiozonatus* is also present in tributaries of the rio Taquari basin, which is biogeographically hybrid, with species shared with rio Paraguai and Amazon basins (Dagosta, de Pinna, 2021). Headwater-capture occurrences were also noted by Melo *et al*. (2022) as a probable cause of this distribution pattern of *Cyphocharax* species from the same region. Because of their correlated geological history, there may be faunal interaction between the Taquari basin and the Araguaia headwaters (Dagosta, de Pinna, 2021). Such events may also enhance *Aequidens* dispersion in the Paraguai and rio Araguaia basins, highlighting the role of hydrogeological theory in this region (Hubert, Henno, 2006; Machado *et al*., 2018). The new species and the new record of *A. plagiozonatus* in the rio Araguaia basin comes from an endemic zone for Characidae,

Callichthyidae, Rivulidae, Aspredinidae, Trichomycteridae, and Curimatidae species (Lima, Moreira, 2003; Dagosta *et al*., 2020; Dagosta, de Pinna, 2021; Melo *et al*., 2022).

Regarding other *Aequidens* species, morphological and ABGD analyses revealed a monophyletic lineage of *A. pallidus* from the rio Jatapu and rio Negro, however GMYC, ABGD and ASAP analyses separated these populations in two species. Using the same delimitation methods, Carvalho *et al*. (2019) identified *A. pallidus* as a non-monophyletic group. In the case of *A. tetramerus*, morphological and PTP analyses suggest that the specimens studied are monophyletic, but the opposite occurs in GMYC, ABGD, and ASAP analyses. The unique specimen of *A. tetramerus* from French Guiana (rio Maroni basin) is distinct from the others from Suriname (rio Paloemeu basin), and they form a polytomy with the *A. epae* clade from Brazil (rio Tapajós basin). This indicates the need for further research into the *Aequidens* specimens found in the vast and interconnected AOG region.

Among the techniques employed herein, distinct scenarios of lineages have been recovered. For instance, for *Cichlasoma paranaense* Kullander, 1983 PTP and ABGD returned one species, while GMYC and ASAP separated into two species. PTP analysis oversplitted some *Aequidens* species, such as *A. plagiozonatus*, *A. epae*, *A. pallidus* and *A. diadema*. Dellicour, Flot (2018) brings out that the size of population data sets influences the delimitation tests, the larger the data set, the lower the chance of correctly delimiting the studied group; on the other hand, when more than 50% of the tests are in agreement, the delimitation is probably correct (Ramirez *et al*., 2023). About distinct delimitation results, *C. paranaense* presented one specimen with a few differences in the sequenced nucleotides, from the upper portion of the rio Paraná basin (rio Grande sub-basin), however, the genetic distance reveals maximum intraspecific values lower than minimum interspecific values, showing the species present the barcoding gap. Same is possible to say about the *Aequidens* species. The perfect congruence among all delimitation methods is not always observed using single-locus approaches (Miralles, Vences, 2013; Dellicour, Flot, 2018). Therefore, the multilocus species approach can be used to support the delimitation study and may be able to handle high rates of speciation and huge population numbers (Dellicour, Flot, 2018). Alternatively, depending on the group studied, phylogenomics might be applied to resolve recent, rapid radiation, revealing even the hybridization cases (Giarla, Esselstyn, 2015; Irisarri *et al*., 2018; Huang *et al*., 2019).

The new species is found in Brazil's Cerrado biome, a biodiversity hotspot that is home to a wide variety of threatened fish species (ICMBio, 2018). Since human activities have had an impact on this area, conservation efforts should focus on strengthening sampling and investigation. This, together with the increased new species descriptions for this region, reinforce the importance of the Cerrado and rio Paraguai basin in the conservation of endemic species.

ACKNOWLEDGMENTS

The Universidade Estadual de Mato Grosso do Sul, the Laboratório de Zoologia da Universidade Federal de Mato Grosso do Sul, the Universidade Estadual de Maringá, Nupélia and PEA provided logistical support. The authors are grateful to Marcos Nunes, Vandergleison Carvalho, Heriberto Gimênes, and Ricardo Rech for the partnership during fieldwork. To Marcelo Britto (MNRJ) for providing the photo of the holotype of *Aequidens rondoni*. To Fernando Carvalho for the general support to LFCT. To Marli Campos and Lais Reia for technical support. To Hans Evers and Heriberto Gimênes for sending images of living specimens of *Aequidens* and also from their collecting sites. To Henrique Varella and to the anonymous reviewer for the valuable suggestions. The Internationale Gemeinschaft Barben Salmler Schmerlen Welse e.V. (Germany), and the Ohio Cichlid Association (USA – 2020 Jim Smith Endowment Fund), plus Steven Grant and Roland van Ouwerkerk provided financial support for collecting trips in the upper rio Correntes basin to LFCT. PROCIENCIA grant 363/2019 supports RB. WJG receives personal grants from Conselho Nacional de Desenvolvimento Científico e Tecnológico (CNPq grants: 305200/2018–6 and 307089/2021–5). RCO is supported by CAPES (grant: 88887.495279/2020–00). CO received financial support from Fundação de Amparo à Pesquisa do Estado de São Paulo (FAPESP grant 2020/13433–6) and CNPq (proc. 306054/2006-0 to CO). GCD is supported by CNPq (grant 151115/2022–2).

REFERENCES

- **Agência Nacional de Águas (ANA).** Relatório de Andamento 03: potenciais impactos de barragens sobre o regime hidrológico nos rios da RH Paraguai. 2019. Available from: https://www.gov.br/ana/pt-br/assuntos/gestao-das-aguas/planos-e-estudos-sobre-rec-hidricos/plano-de-recursos-hidricos-rio-paraguai/relatorio-final-de-diagnostico_hidrologia_parte1.pdf
- **Aquino PPU, Colli GR.** Headwater captures and the phylogenetic structure of freshwater fish assemblages: a case study in central Brazil. J Biogeog. 2017; 44(1):207–16. https://doi.org/10.1111/jbi.12870
- **Barel CDN, Van Oijen MJP, Witte F Witte-Maas ELS.** An introduction to the taxonomy and morphology of the haplochromine Cichlidae from Lake Victoria. Netherl J Zool. 1976; 27(4):333–80.
- **Carvalho APC, Collins RA, Martínez JG, Farias IP, Hrbek T.** From shallow to deep divergences: mixed messages from Amazon Basin cichlids. Hydrobiologia. 2019; 832:317–29. https://doi.org/10.1007/s10750-018-3790-x
- **Carvalho DC, Oliveira DAA, Pompeu PS, Leal CG, Oliveira C, Hanner R.** Deep barcode divergence in Brazilian freshwater fishes: the case of the São Francisco River basin. Mitoch DNA. 2011; 22:80–86. https://doi.org/10.3109/19401736.2011.588214
- **Dagosta FCP, de Pinna M.** Two new catfish species of typically Amazonian lineages in the Upper Rio Paraguay (Aspredinidae: Hoplomyzontinae and Trichomycteridae: Vandelliinae), with a biogeographic discussion. Pap Avulsos Zool. 2021; 61:e20216147. https://doi.org/10.11606/1807-0205/2021.61.47
- **Dagosta FCP, de Pinna M.** Biogeography of Amazonian fishes: deconstructing river basins as biogeographic units. Neotrop Ichthyol. 2017; 15(3):e170034. https://doi.org/10.1590/1982-0224-20170034
- **Dagosta FCP, de Pinna M, Peres CA, Tagliacollo VA.** Existing protected areas provide a poor safety-net for threatened Amazonian fish species. Aquat Conserv Mar Fresh Ecosys. 2020; 31(5):1167–89. https://doi.org/10.1002/aqc.3461

- **Dellicour S, Flot J-F.** The hitchhiker's guide to single-locus species delimitation. Mol Ecol Res. 2018; 18(6):1234–46. https://doi.org/10.1111/1755-0998.12908
- **Deprá GC, Ohara WM, Silva HP.** *Geophagus pyrineusi*: a new species from the rio Teles Pires, rio Tapajós basin, Brazil (Cichliformes: Cichlidae: Geophagini). Zootaxa. 2022; 5153(1):37–53. https://doi.org/10.11646/zootaxa.5162.1.2
- **Deprá GC, Ota RR, Vitorino Júnior OB, Ferreira KM.** Two new species of *Knodus* (Characidae: Stevardiinae) from the upper rio Tocantins basin, with evidence of ontogenetic meristic changes. Neotrop Ichthyol. 2021; 19(1):e200106. https://doi.org/10.1590/1982-0224-2020-0106
- **Drummond AJ, Suchard MA, Xie D, Rambaut A.** Bayesian phylogenetics with BEAUTi and the BEAST 1.7. Mol Biol Evol. 2012; 29(8):1969–73. https://doi.org/10.1093/molbev/mss075
- **Fricke R, Eschmeyer WN, Van der Laan R.** Eschmeyer's catalog of fishes: genera, species, references [Internet]. San Francisco: California Academy of Science. 2024; Available from: http://researcharchive.calacademy.org/research/ichthyology/catalog/fishcatmain.asp
- **Fujisawa T, Barraclough TG.** Delimiting species using single-locus data and the Generalized Mixed Yule Coalescent (GMYC) approach: A revised method and evaluation on simulated data sets. Syst Biol. 2013; 62(5):707–24. https://doi.org/10.1093/sysbio/syt033
- **Giarla TC, Esselstyn JA.** The challenges of resolving a rapid, recent radiation: empirical and simulated phylogenomics of Philippine shrews. Syst Biol. 2015; 64(5):727–40. https://doi.org/10.1093/sysbio/syv029
- **Garavello JC, Ramirez JL, Oliveira AK, Britski HA, Birindelli JLO, Galetti Jr. PM.** Integrative taxonomy reveals a new species of Neotropical headstanding fish in genus *Schizodon* (Characiformes: Anostomidae). Neotrop Ichthyol. 2021; 19(4):e210016. https://doi.org/10.1590/1982-0224-2021-0016
- **Gimênes Júnior H, Rech R.** Guia ilustrado dos peixes do Pantanal e entorno. Campo Grande: Julien Design; 2022.
- **Gomes LC, Pessali TC, Sales NG, Pompeu PS, Carvalho DC.** Integrative taxonomy detects cryptic and overlooked fish species in a neotropical river basin. Genetica. 2015; 143:581–88. https://doi.org/10.1007/s10709-015-9856-z
- **Hernández-Acevedo JH, Machado-Allison A, Lasso CA.** *Aequidens superomaculatum* (Teleostei: Cichlidae) una nueva especie del alto Orinoco y Río Negro, Venezuela. Biota Colomb. 2015; 16(2):96–106.
- **Huang X-C, Su J-H, Ouyang J-X, Ouyang S, Zhou C-H, Wu X-P.** Towards a global phylogeny of freshwater mussels (Bivalvia: Unionida): Species delimitation of Chinese taxa, mitochondrial phylogenomics, and diversification patterns. Mol Phylogenet Evol. 2019; 130:45–59. https://doi.org/10.1016/j.ympev.2018.09.019
- **Hubert N, Renno J-F.** Historical biogeography of South American freshwater fishes. J Biogeogr. 2006; 33(8):1414–36. https://doi.org/10.1111/j.1365-2699.2006.01518.x
- **Instituto Chico Mendes de Conservação da Biodiversidade (ICMBio).** Livro vermelho da fauna brasileira ameaçada de extinção: Volume VI - Peixes. Brasília: ICMBio/MMA; 2018. Available from: https://www.gov.br/icmbio/pt-br/centrais-de-conteudo/publicacoes/publicacoes-diversas/livro_vermelho_2018_vol6.pdf
- **Ilves KL, Torti D, López-Fernández H.** Exon-based phylogenomics strengthens the phylogeny of Neotropical cichlids and identifies remaining conflicting clades (Cichliformes: Cichlidae: Cichlinae). Mol Phylogenetic Evol. 2018; 118:232–43. https://doi.org/10.1016/j.ympev.2017.10.008
- **Irisarri I, Singh P, Koblmüller S, Torres-Dowdall J, Henning F, Franchini P *et al*.** Phylogenomics uncovers early hybridization and adaptive loci shaping the radiation of Lake Tanganyika cichlid fishes. Nat Commun. 2018; 9(1):3159. https://doi.org/10.6084/m9.figshare.6182519
- **International Union for Conservation of Nature (IUCN). Standards and petitions committee.** Guidelines for using the IUCN Red List categories and criteria. Version 15.1 [Internet]. Gland; 2022. Available from: http://www.iucnredlist.org/documents/RedListGuidelines.pdf

- **Ivanova NV, Dewaard JR, Hebert PDN.** An inexpensive, automation-friendly protocol for recovering high-quality DNA. Mol Ecol Notes. 2006; 6(4):998–1002. https://doi.org/10.1111/j.1471-8286.2006.01428.x
- **Jennings WB, Ruschi PA, Ferraro G, Quijada CC, Silva-Malanski ACG, Prosdocimi F *et al*.** Barcoding the Neotropical freshwater fish fauna using a new pair of universal COI primers with a discussion of primer dimers and M13 primer tails. Genome. 2019; 62(2):77–83. https://doi.org/10.1139/gen-2018-0145
- **Kimura M.** A simple method for estimating evolutionary rates of base substitutions through comparative studies of nucleotide sequences. J Mol Evol. 1980; 16(2):111–20. https://doi.org/10.1007/BF01731581
- **Kullander SO.** A revision of the South American cichlid genus *Cichlasoma* (Teleostei: Cichlidae). Stockholm: Naturhistoriska Riksmuseet. 1983.
- **Kullander SO.** Cichlid fishes from the La Plata basin. Part V. Description of *Aequidens plagiozonatus* sp. n. (Teleostei, Cichlidae) from the Paraguay River system. Zool Scripta. 1984; 13(2):155–59. https://doi.org/10.1111/j.1463-6409.1984.tb00031.x
- **Kullander SO.** Cichlid fishes of the Amazon River drainage of Peru. Swedish Museum of Natural History, Stockholm; 1986.
- **Kullander SO.** Three new cichlid species from southern Amazonia: *Aequidens gerciliae*, *A. epae* and *A. michaeli*. Ichthyol Explor Freshw. 1995; 6(2):149–70.
- **Kullander SO.** A phylogeny and classification of the South American Cichlidae (Teleostei: Perciformes). In: Malabarba LR, Reis RE, Vari RP, Lucena ZMS, Lucena CAS, editors. Phylogeny and classification of Neotropical fishes. Porto Alegre: Edipucrs; 1998. p.461–98.
- **Kullander SO.** Family Cichlidae (Cichlids). In: Reis RE, Kullander SO, Ferraris Jr. CJ, editors. Check list of the freshwater fishes of South and Central America. Porto Alegre: Edipucrs; 2003. p.606–54.
- **Kullander SO.** *Krobia xinguensis*, a new species of cichlid fish from the Xingu River drainage in Brazil (Teleostei: Cichlidae). Zootaxa. 2012; 3197(1):43–54. https://doi.org/10.11646/zootaxa.3197.1.2
- **Kullander SO, Nijssen H.** The cichlids of Surinam (Teleostei: Labroidei). E. J. Brill, Leiden; 1989.
- **Kumar S, Stecher G, Li M, Knyaz C, Tamura K.** MEGA X: molecular evolutionary genetics analysis across computing platforms. Mol Biol Evol. 2018; 35(6):1547–49. https://doi.org/10.1093/molbev/msy096
- **Lima FC, Moreira CR.** Three new species of *Hyphessobrycon* (Characiformes: Characidae) from the upper rio Araguaia basin in Brazil. Neotrop Ichthyol. 2003; 1(1):21–33. https://doi.org/10.1590/S1679-62252003000100003
- **Machado CB, Galetti Jr. PM, Carnaval AC.** Bayesian analyses detect a history of both vicariance and geodispersal in Neotropical freshwater fishes. J Biogeogr. 2018; 45(6):1313–25. https://doi.org/10.1111/jbi.13207
- **Melo BF, Tencatt LF, Oliveira C.** Phylogenetic evidence for the *Cyphocharax saladensis* clade with description of a new species of *Cyphocharax* endemic to the upper rio Paraguai basin (Teleostei: Curimatidae). Ichthyol Herpetol. 2022; 110(2):327–39. https://doi.org/10.1643/i2021057
- **Miralles A, Vences M.** New metrics for comparison of taxonomies reveal striking discrepancies among species delimitation methods in Madascincus lizards. PLoS ONE. 2013; 8(7):e68242. https://doi.org/10.1371/journal.pone.0068242
- **Musilová Z, Říčan O, Janko K, Novák J.** Molecular phylogeny and biogeography of the Neotropical cichlid fish tribe Cichlasomatini (Teleostei: Cichlidae: Cichlasomatinae). Mol Phylogenet Evol. 2008; 46(2):659–72. https://doi.org/10.1016/j.ympev.2007.10.011
- **Musilová Z, Říčan O, Novák J.** Phylogeny of the Neotropical cichlid fish tribe Cichlasomatini (Teleostei: Cichlidae) based on morphological and molecular data, with the description of a new genus. J Zool Syst Evol Res. 2009; 47(3):234247. https://doi.org/10.1111/j.1439-0469.2009.00528.x
- **Ota RR, Deprá GC, Kullander S, Graça WJ, Pavanelli CS.** A new species of *Satanoperca* (Teleostei: Cichlidae) from the rio Tocantins basin, Brazil. Neotrop Ichthyol. 2021; 19(4):e210116. https://doi.org/10.1590/1982-0224-2021-0116
- **Padial JM, Miralles A, De la Riva I, Vences M.** The integrative future of taxonomy. Front Zool. 2010; 7:16. https://doi.org/10.1186/1742-9994-7-16

- **Pereira LHG, Hanner R, Foresti F, Oliveira C.** Can DNA barcoding accurately discriminate megadiverse Neotropical freshwater fish fauna? BMC Genetics. 2013; 14:20. https://doi.org/10.1186/1471-2156-14-20
- **Pereira LHG, Maia GMG, Hanner R, Foresti F, Oliveira C.** DNA barcodes discriminate freshwater fishes from the Paraíba do Sul River Basin, São Paulo, Brazil. Mitoch DNA. 2011a. 22:71–79. https://doi.org/10.3109/19401736.2010.532213
- **Pereira LHG, Pazian MF, Hanner R, Foresti F, Oliveira C.** DNA barcoding reveals hidden diversity in the Neotropical freshwater fish *Piabina argentea* (Characiformes: Characidae) from the Upper Paraná Basin of Brazil. Mitoch DNA. 2011b; 22:87–96. https://doi.org/10.3109/19401736.2011.588213
- **Pons J, Barraclough TG, Gomez-Zurita J, Cardoso A, Duran DP, Hazell S *et al*.** Sequence-based species delimitation for the DNA taxonomy of undescribed insects. Syst Biol. 2006; 55(4):595–609. https://doi.org/10.1080/10635150600852011
- **Puillandre N, Brouillet S, Achaz G.** ASAP: assemble species by automatic partitioning. Mol Ecol Res. 2021; 21(2):609–20. https://doi.org/10.1111/1755-0998.13281
- **Puillandre N, Lambert A, Brouillet S, Achaz G.** ABGD, automatic gap discovery for primary species delimitation. Mol Ecol. 2012; 21(8):1864–77. https://doi.org/10.1111/j.1365-294X.2011.05239.x
- **Rambaut A.** FigTree-Version 1.4. 4, a graphical viewer of phylogenetic trees. Computer program distributed by the author. 2019. Available from: http://tree.bio.ed.ac.uk/software/figtree
- **Rambaut A, Drummond AJ, Xie D, Baele G, Suchard MA.** Posterior summarization in Bayesian phylogenetics using Tracer 1.7. Syst Biol. 2018; 67(5):901–04. https://doi.org/10.1093/sysbio/syy032
- **Ramirez JL, Valdivia P, Rosas-Puchuri U, Valdivia NL.** SPdel: A pipeline to compare and visualize species delimitation methods for single-locus datasets. Mol Ecol Res. 2023; 23(8):1959–65. https://doi.org/10.1111/1755-0998.13864
- **Reis RB, Frota A, Deprá GC, Ota RR, Graça WJ.** Freshwater fishes from Paraná State, Brazil: an annotated list, with comments on biogeographic patterns, threats, and future perspectives. Zootaxa. 2020; 4868(4):451–94. https://doi.org/10.11646/ZOOTAXA.4868.4.1
- **Říčan O, Musilová Z, Muška M, Novák J.** Development of coloration patterns in Neotropical cichlids (Teleostei: Cichlidae: Cichlasomatinae). Folia Zool. 2005; 54:1–46.
- **Souza CR, Affonso PRAM, Bitencourt JA, Sampaio I, Carneiro PLS.** Species validation and cryptic diversity in the *Geophagus brasiliensis* Quoy & Gaimard, 1824 complex (Teleostei, Cichlidae) from Brazilian coastal basins as revealed by DNA analyses. Hydrobiologia. 2018; 809:309–321. https://doi.org/10.1007/s10750-017-3482-y
- **Secretaria de Estado do Meio Ambiente (SEMA).** Relatório de qualidade das águas superficiais da bacia do alto Paraguai/MS 2004. Campo Grande, Mato Grosso do Sul. Secretaria de Estado do Meio Ambiente e Recursos Hídricos. 2005. Available from: http://www.servicos.ms.gov.br/imasuldownloads/relatorios/2004/relatorio2004.pdf
- **Van der Sleen P, Albert JS.** Field guide to the fishes of the Amazon, Orinoco & Guianas. New Jersey: Princeton University Press; 2018.
- **Taylor WR, Van Dyke GC.** Revised procedures for staining and clearing small fishes and other vertebrates for bone and cartilage study. Cybium. 1985; 9(2):107–19. Available from: https://sfi-cybium.fr/en/node/2423
- **Thompson JD, Higgins DG, Gibson TJ.** CLUSTAL W: improving the sensitivity of progressive multiple sequence alignment through sequence weighting, position-specific gap penalties and weight matrix choice. Nucleic Acids Res. 1994; 22(22):4673–80. https://doi.org/10.1093/nar/22.22.4673
- **Xia X, Xie Z.** DAMBE: software package for data analysis in molecular biology and evolution. J Hered. 2001; 92(4):371–73. https://doi.org/10.1093/jhered/92.4.371
- **Zhang J, Kapli P, Pavlidis P, Stamatakis A.** A general species delimitation method with applications to phylogenetic placements. Bioinformatics. 2013; 29(22):2869–76. https://doi.org/10.1093/bioinformatics/btt499

AUTHORS' CONTRIBUTION

Rianne Caroline de Oliveira: Formal analysis, Writing-original draft, Writing-review and editing.
Luiz Fernando Caserta Tencatt: Conceptualization, Formal analysis, Funding acquisition, Project administration, Writing-original draft, Writing-review and editing.
Gabriel de Carvalho Deprá: Formal analysis, Writing-original draft, Writing-review and editing.
Ricardo Britzke: Formal analysis, Project administration, Writing-original draft, Writing-review and editing.
Claudio Oliveira: Formal analysis, Funding acquisition, Project administration, Writing-original draft, Writing-review and editing.
Weferson Júnio da Graça: Conceptualization, Formal analysis, Funding acquisition, Project administration, Writing-original draft, Writing-review and editing.

ETHICAL STATEMENT

The description of the new species is part of the project: "Sistemática, taxonomia e biogeografia de ciclídeos neotropicais" (#305200/2018–6 CNPq and # 4937/2020 UEM) registered in SisGen n° A954837 to WJG. The specimens were collected with authorizations #73139–3, #73139–2, and #45578–7 sent by Sistema de Autorização e Informação em Biodiversidade (SISBio) to LFCT.

COMPETING INTERESTS

The author declares no competing interests.

HOW TO CITE THIS ARTICLE

- **Oliveira RC, Tencatt LFC, Deprá GC, Britzke R, Oliveira C, Graça WJ.** A new species of *Aequidens* (Cichliformes: Cichlidae) from the rio Paraguai basin, Brazil. Neotrop Ichthyol. 2024; 22(2):e230106. https://doi.org/10.1590/1982-0224-2023-0106

Neotropical Ichthyology

OPEN ACCESS

Official Journal of the
Sociedade Brasileira de Ictiologia
SBI